Design and Optimization of an All Optically Driven Phase Correction MEMS Deformable Mirror Device using Finite Element Analysis

V. Mathur*[1], K. Anglin[1], V.S. Prasher[1], K. Termkoa[1], S.R.Vangala[1], X. Qian[1], W.D. Goodhue[1] J. Sherwood[2], B. Haji-Saeed[3], J. Khoury[3]
[1]Photonics Center, Department of Physics and Applied Physics, University of Massachusetts, Lowell, MA-01851 , [2] Department of Mechanical Engineering , University of Massachusetts, Lowell, [3]Air Force Research Laboratory/Sensors Directorate, Hanscom AFB, MA-01731
*Corresponding Author: One University Avenue, Lowell, MA-01854,USA, vaibhav_mathur@student.uml.edu

Abstract: Optically addressable MEMS mirrors are required for future high density adaptive optics array systems. We have demonstrated a novel technique of achieving this by actuating low stress Silicon Nitride micro mirrors via cascaded wafer bonded Gallium Arsenide photo detectors on Gallium Phosphide. In the work reported here, we discuss the key design parameters of the device, and present the finite element method simulation results using COMSOL Multiphysics package to optimize the devices.

Keywords: Adaptive optics, Optical MEMS, micro mirrors, wafer bonding, GaAs PIN diodes.

1. Introduction

Adaptive optics devices for signal processing and atmospheric turbulence correction require MEMS micro mirrors as they are key enabling components. Most current systems are electrically addressed, but future applications require optically as well as individually addressable arrays of such devices **[1].** In the current work we develop a novel device that involves integrating silicon nitride micro mirrors via thin film resistors to wafer bonded GaAs (Gallium Arsenide) P-I-N diodes on a transparent GaP (Gallium Phosphide) back plane.

A single pixel of the final device is illustrated in figure 1(a). The GaAs PIN photo diode is addressed by focusing laser light through the transparent GaP. The photocurrent then passes through the tantalum nitride thin film resistor via conductive SU-8 pillars **[2]**. The operation points of the device are shown in figure 1(b). When no light is applied to the PIN pixel, no voltage is dropped across the spring plate (point A). When light is applied to the pixel, the photocurrent causes the operation point to move to the intersection of diode and resistor I-V curves (point B), thus actuating the plate.

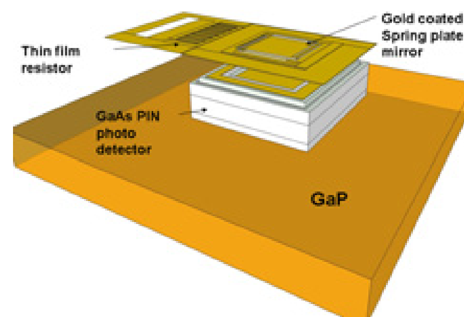

(a)

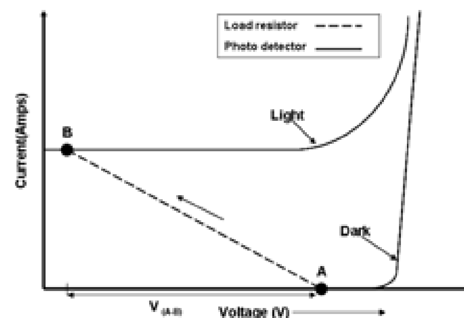

(b)

Figure 1. (a) Schematic of the silicon nitride spring plate cascaded on top of the wafer bonded GaAs PIN photo detector in the final device **(b)** Operation points on the I-V plots

2. Use of COMSOL Multiphysics

The ease of actuation of a silicon nitride mirror is critically dependent on its geometry and

thickness. To optimize these parameters, force vs deflection, and voltage vs deflection studies were carried out by coupling the electrostatics and structural mechanics modules of COMSOL Multiphysics. These were compared to actual nano-indentation and interferometer results of the device.

The GaAs P-I-N photo diodes used in this device were epitaxially grown, mesa etched, and experimentally characterized for breakdown and photo response. A COMSOL model coupling the electrostatics module with the convection and diffusion module was then developed to extract the current voltage characteristics, and to compare with the measured values to aid in future design changes.

Also, an important fabrication step in this device involves bonding GaAs P-I-N grown wafers to GaP back substrates. This requires a custom designed high stress, high temperature wafer bonding fixture. Here too, FEM studies of the thermal mechanical interactions using COMSOL Multiphysics package were used to optimize the design parameters.

3. Spring Plate Design

The phase correction application in our adaptive optics system requires a movable MEMS mirror with piston motion in the vertical direction of the order of half wavelength (≈ half micron). A spring plate design consisting of gold coated thin Si_3N_4 films with four fixed arms was found to be most suitable for dynamic corrections involving high frequency applications **[3]**. The Si_3N_4 in our device was deposited using a low stress yielding mixed frequency recipe on the PECVD (Pressure Enhance Chemical Vapor Deposition) system **[4].** A nano mechanical analyzer (Hysitron, Inc.) was used to do multiple indents on a one micron thick layer of Si_3N_4 on a Si substrate and the Young's modulus and hardness were extracted using a bilayer interpolation method **[5].** Young's modulus in the range of 250-270 GPa was determined by this technique which was very close to earlier reported values for such PECVD films **[6].**

Using the mechanical characterization data obtained, a COMSOL model with about half micron thick spring plate structure was indented and the resulting displacements calculated for varying loads. The load vs displacement data was seen to agree well with actual indentations on the spring plates, and a spring constant of approximately 0.98 N/m was determined. Figure 2(a) shows a deformed spring plate under one micro newton force load. Figure 2(b) shows both experimental and simulation plot of load vs displacement. The curves are found to agree well except at higher displacements, which can be attributed to slight variations in Young's modulus due to residual stresses and process conditions.

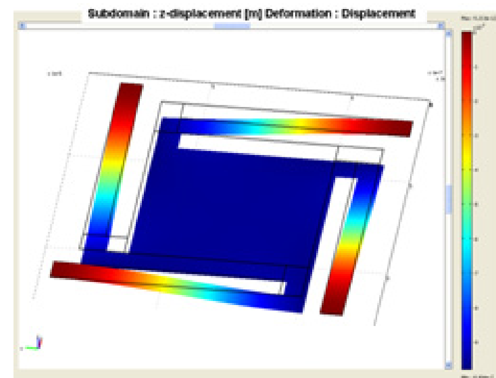

(a)

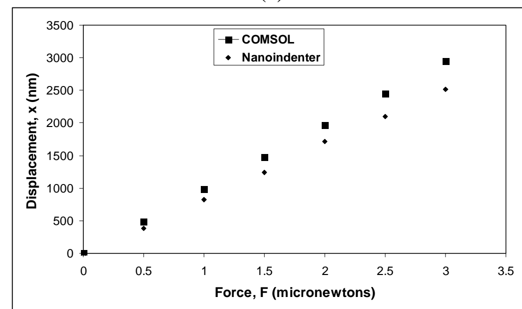

(b)

Figure 2. Load vs displacement studies (a) COMSOL simulation showing a displacement of 980nm for a face load of one micron (b) Comparison of the load vs displacement curves, both experimental and simualtion

A similar study was then carried out to determine the voltage vs displacement characteristics of these mirrors. The electrostatics module was added to the earlier model and a parallel plate below the spring plate defined as the lower electrode. The bottom plate was defined with a two micron spacing to simulate the actual device with two micron high SU-8 support pillars separating the mirrors from the cascaded photo detectors.

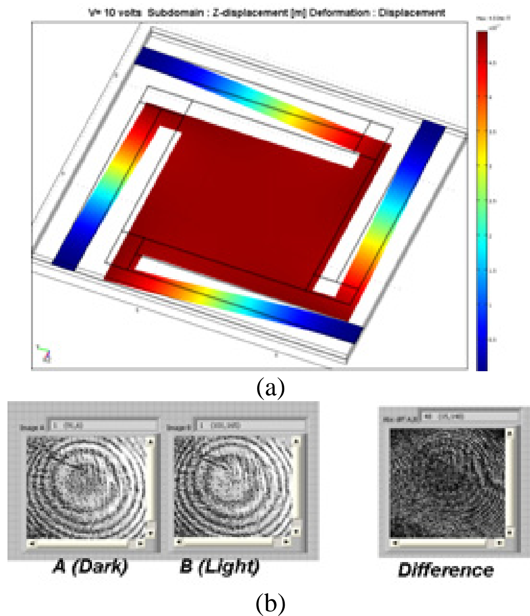

(a)

(b)

Figure 3. Simulation and experimental characterization (a) COMSOL model showing a electrostatic actuation of about half wavelength at 10 volts (b) Intereference pattern showing a clear fringe shift at 10 volts on actual sample.

The simulation results as illustrated in figure 3(a), show that a voltage of eight to ten volts is sufficient to cause approximately 500nm displacement of the spring plate mirrors. A Michelson interferometer setup with 632nm Helium Neon laser **[7]** was used to verify this spring plate actuation. Figure 3(b) shows CCD captured snapshots of the interference pattern both under dark condition and under illumination. The difference clearly shows a fringe shift caused by a 830nm laser beam focused on the GaAs PIN diode, and causing a voltage drop of ten volts via an external resistor.

4. PIN diode design

As discussed in the previous section, the maximum voltage contrast across the spring plate mirrors achieved is dependent on the current voltage characteristics of the cascaded GaAs PIN diode both under dark and illuminated conditions. As these photo diodes are operated under reverse bias, their breakdown voltage is required to be greater than the achievable voltage drop across the mirror. Based on the spring plate studies shown, a breakdown voltage of 25-30 volts is hence desirable for our device.

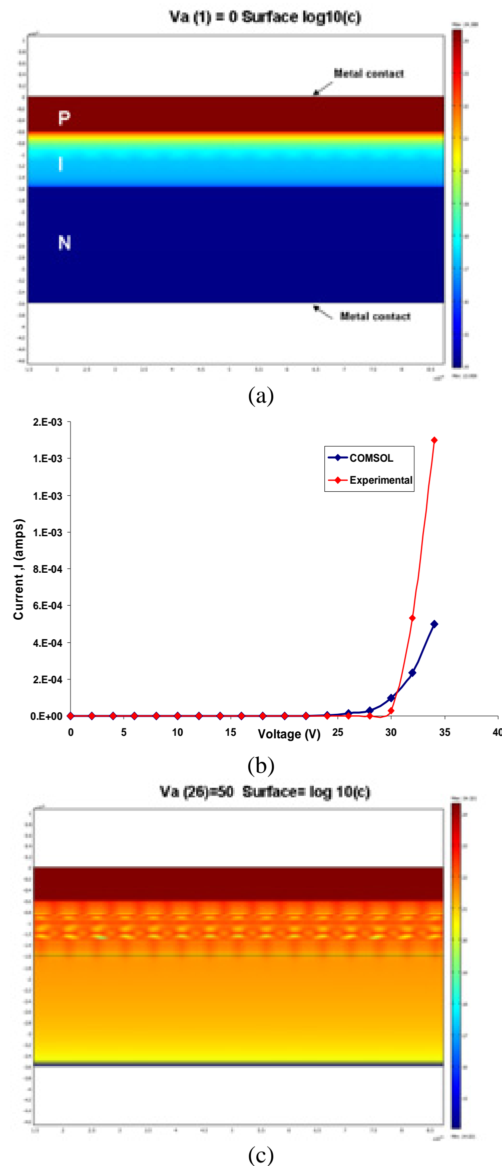

(a)

(b)

(c)

Figure 4. GaAs PIN diode breakdown voltage simulation (a) Hole distribution at equilibrium (V = 0Volts) (b) Experimental and COMSOL simulation I-V curves of a GaAs PIN diode. (c) Hole distribution after breakdown (V = 50volts)

The GaAs PINs being modeled here were grown epitaxially, enabling precise control of the doping levels and thicknesses of the P, I and N epilayers. In our COMSOL model, the thicknesses of these epilayers were modeled close to our current MBE (molecular beam

epitaxy) growth design of 0.6, 1 and 2 microns respectively.

A uniform doping profile was assumed in the three layers. The upper and lower boundary layers were defined as the biasing electrodes in the electrostatics module, and the resulting electron-hole profile solved using the convection-diffusion model. The breakdown voltage in each case was determined from the current voltage characteristics extracted by integrating the normal components of the current density over the sub domains.

Figure 3(a) shows the COMSOL simulation of one such epistructure, with the metal contacts defined on either side. The image shows the hole distribution across the device at equilibrium (no bias voltage). The I-V characteristics of the junction exhibit a clear breakdown at about 30 volts, as can be seen from the simulation and experimental data in figure 4(b). Figure 4(c) shows a plot of the hole distribution in the epistructure after breakdown, the migration of the majority charge carries can be easily seen.

Breakdown characteristics of GaAs abrupt P-N junctions have been well studied [8]. Here some further studies were carried out to determine the relation of doping concentrations and breakdown voltage in the PIN junctions. The doping concentrations in these cases were varied in the P and N regions from 3E+17 to 3E+18 cm^{-3}, keeping the n-type lightly doped I layer constant at 1E+15 cm^{-3}. As shown in figure 5(a), the breakdown voltage is seen to reduce following a power law with increasing doping levels. The cross marks on the plot show the doping levels of our current design measured experimentally, exhibiting breakdown close to 30 volts.

Similarly, as illustrated in figure 5(b) , a plot of the intrinsic layer thickness vs break down voltage shows a linear variation, keeping the doping concentration constant at 2E+18 cm^{-3}. These studies have helped in successfully verifying our current design, and will thus aid in future design improvements.

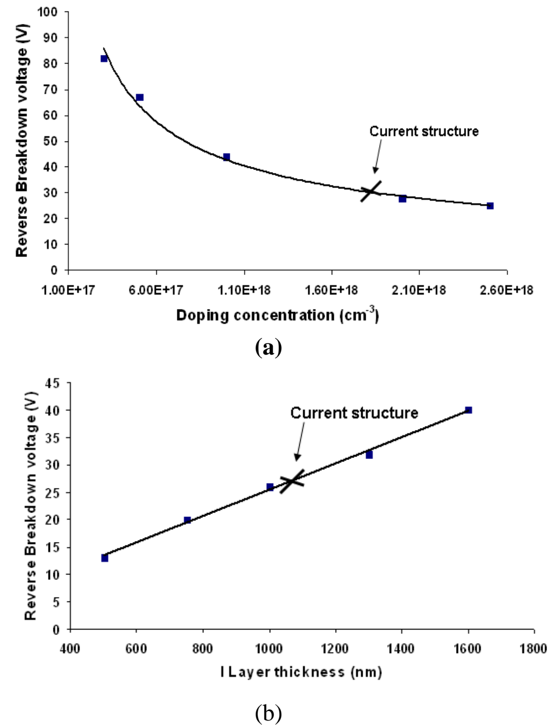

(b)

Figure 5. Breakdown voltage studies of the GaAs PIN diodes using COMSOL (a) Plot showing breakdown voltage as a function of doping concentration levels, with constant intrinsic layer thickness (b) Plot showing breakdown voltage vs intrinsic layer thickness, with constant doping concentrations.

5. Wafer bonding

An important device fabrication step involves transferring GaAs PINs to the GaP back substrate. This is achieved, by wafer bonding the two samples face to face in a custom designed furnace and fixture. Figure 6(a) shows a 3-D image of the fixture arrangement. Samples to be bonded are sandwiched between two graphite pieces, and slid under a glass tube. The tightness is adjusted using thin shims of graphite.

This fixture arrangement is heated up to 700°C in the furnace. The thermal stresses due to expansion coefficient mismatch between graphite and glass initiates sample bonding under high stresses. Figure 6(b) shows thermal failure of a glass tube at 700°C in one of our earlier designs.

(a) (b)

Figure 6. Bonding fixture (a) 3-D schematic illustrating the tube and fixture design (b) Glass tube thermal failure.

A COMSOL model as shown in figure 7(a) utilizing contact boundary conditions between the graphite and glass tube was solved in the thermal structural module. The temperature was ramped up to 700 degrees and the normal stresses plotted as shown in figure 7(b). These thermal-structural FEM simulations revealed high stress concentrations due to the elliptical expansion of the graphite fixture, which ultimately led to breakage.

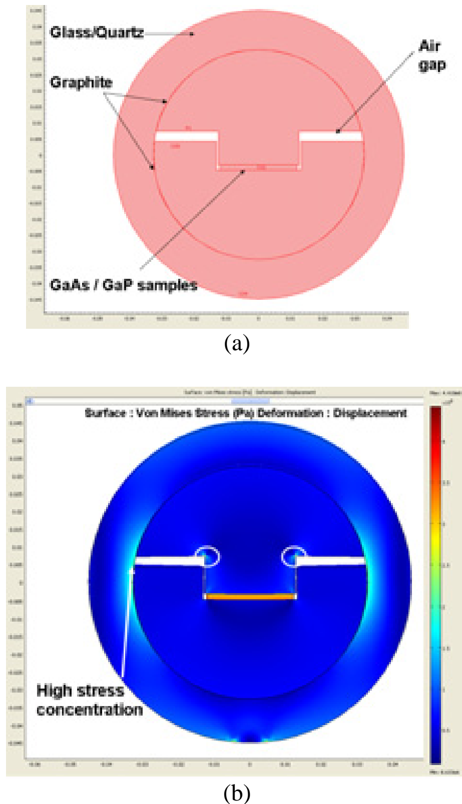

(a)

(b)

Figure 7. Preliminary fixture design, and resulting stresses (a) Sketch showing tight fit between the graphite and glass tube. (b) Thermal structural simulation showing high stress concentrations on the glass tube.

To allow more freedom of expansion and lower stress concentrations, a number of design changes were attempted. Minimum stress concentration was observed when the radius of curvature of the upper and lower graphite fixtures was reduced, as shown in figure 8(a). This allowed greater freedom of expansion leading to slightly elliptical shape, enabling higher normal stresses on the sample surface, as can be seen from figure 8(b).

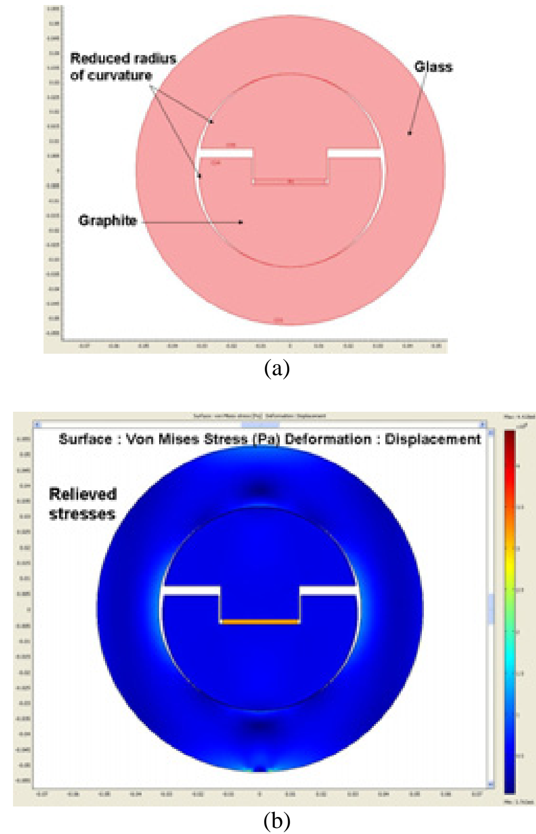

(a)

(b)

Figure 8. Modified fixtures design (a) Reduced radius of curvatures of the graphite fixtures (b) Thermal structural simulation results showing slightly elliptical deformation, and lower stress concentration.

From these studies, stresses of the order of about 300 MPa are estimated to be acting on the wafers during bonding. The design changes implemented from these studies eliminated the thermal failures, and also led to a more defect free bonding interface. Successfully bonded GaAs PINs on GaP were patterned and mesas were fabricated as shown in figure 8. These bonded PINs were tested and found to have the

same breakdown voltage as non bonded PINs with a lower photo response.

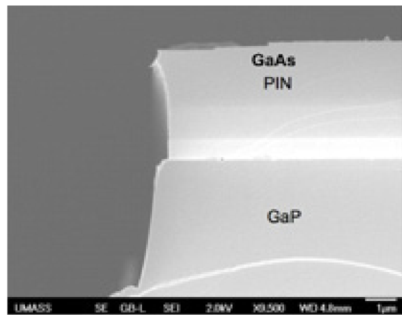

Figure 8 . SEM image of a successfully bonded and patterned GaAs PIN mesa on GaP

6. Conclusions and future work

In conclusion, based on the above FEM studies, the process and design parameters of. Si_3N_4 spring plate mirror, GaAs PIN diode and wafer bonding process were optimized which led to a working prototype of our MEMS adaptive optics device.

In the future, we will attempt to simulate the photo response of our PIN diodes and its dependence on parameters such as mesa width, and incident optical power. Spring plate structures with thicker but smaller dimensions will also be explored to increase the fill factor of our devices.

7. Acknowledgements

This work was supported by the United States Air Force under contract # FA8718-05-C0081. The opinions, interpretations, conclusions and recommendations are those of the authors and not necessarily those of the United States Air Force.

8. References

1.Bifano et. al. “Microelectromechanical Deformable Mirrors”, IEEE Journal of Selected Topics in Quantum Electronics **Volume 5** No.1 Jan/Feb Page 83-89 (1999)

2.V.Mathur et. al. “All optically driven MEMS mirrors via direct cascading with wafer bonded GaAs/GaP PIN photodetectors” In proceedings of *IEEE LEOS Optical MEMS and Nanophotonics Conference,Florida,USA* (2009)

3.G.Griffith et. al. “Patterned multipixel membrane MEMS optically addressed spatial light modulator with megahertz response” *IEEE Photonics Technology Letters* **Volume 19** No.3 Page 173-175 (2007)

4.A Tarraf et. al. “Stress investigation of PECVD dielectric layers for advanced optical MEMS” *J. Micromech. Microeng*. **Volume 14** Page 317-323 (2004)

5.H. Huang et. al. “Characterization of mechanical properties of silicon nitride thin films for MEMS devices by nanoindentation” *J. Matr. Sci. Technol.* **Volume 21** Suppl. (2005)

6.J. Taylor “The mechanical properties and microstructure of plasma enhanced chemical vapor deposition silicon nitride thin films” J. Vac. Sci. Technol. **Volume 9** page 2464-2468 (1991)

7.B.Haji-Saeed et. al. “Photoconductive optically driven deformable membrane under high frequency bias : fabrication , characterization and modelling” *Applied optics*, **Volume 45** No.14 ,Page 3226-3236 (2006)

8.*http://www.ioffe.rssi.ru/SVA/NSM/Semicond/GaAs/electric.html* (last checked on 09/09/09)